Available online at www.sciencedirect.com
SCIENCE DIRECT®
Physica D 207 (2005) 24–40
PHYSICA D
www.elsevier.com/locate/physd

Resampling hierarchical processes in the wavelet domain: A case study using atmospheric turbulence

Claudia Angelini[a], Daniela Cava[b,*], Gabriel Katul[c], Brani Vidakovic[d]

[a] *Istituto per le Applicazioni del Calcolo "Mauro Picone", Sezione di Napoli, Consiglio Nazionale delle Ricerche, Italy*
[b] *Istituto di Scienze dell'Atmosfera e del Clima, Sezione di Lecce, CNR 73100, Lecce, Italy*
[c] *Nicholas School of the Environment and Earth Sciences, Duke University, Durham, NC 27708-0328, USA*
[d] *Georgia Institute of Technology, Atlanta, GA 30332-0205, USA*

Received 20 May 2004; received in revised form 6 May 2005; accepted 11 May 2005
Available online 13 June 2005
Communicated by M. Vergassola

Abstract

There is a growing need for statistical methods that generate an ensemble of plausible realizations of a hierarchical process from a single run or experiment. The main challenge is how to construct such an ensemble in a manner that preserves the internal dynamics (e.g. intermittency) and temporal persistency. A popular hierarchical process often used as a case study in such problems is atmospheric turbulent flow. Analogies to turbulence are often called upon when information flow from large to small scales, non Gaussian statistics, and intermittency are inherent attributes of the hierarchical process under consideration. These attributes are key defining syndromes of the turbulent cascade thereby making turbulence time series ideal for testing such ensemble generation schemes. In this study, we propose a wavelet based resampling scheme (WB) and compare it to the traditional Fourier based phase randomization bootstrap (FB) approach within the context of the turbulence energy cascade. The comparison between the two resampling methods and observed ensemble statistics constructed by clustering similar meteorological conditions demonstrate that the WB reproduces several features related to intermittency of the ensemble series when compared to FB. In particular, the WB exhibited an increase in wavelet energy activity and an increase in the wavelet flatness factor with increasing frequency consistent with the cluster of ensemble statistics. On the other hand, the FB yielded no increase in such energy activity with scale and resulted in near Gaussian wavelet coefficients at all frequencies within the inertial subrange. The scaling behavior of the longitudinal (u') and vertical (w') velocity structure functions of various order $p > 0$ confirms that WB preserves the small scale intermittency, whereas FB completely destroys it. The extension of WB to the multivariate case is also demonstrated via the conservation of co-spectra between u' and w' time series. Because the resampling strategy proposed here is conducted in the wavelet domain, gap-infected and uneven sampled time series can be readily accommodated within the WB. Finally, recommendations about the filter and block sizes are discussed.

Keywords: Ergodicity; Hierarchical processes; Intermittency; Resampling; Turbulence; Wavelets

* Corresponding author. Tel.: +39 0832 298721; fax: +39 0832 298716.
E-mail address: d.cava@isac.cnr.it (D. Cava).

0167-2789/$ – see front matter © 2005 Elsevier B.V. All rights reserved.
doi:10.1016/j.physd.2005.05.015

1. Introduction

Stochastic processes that exhibit hierarchical information flow from long to short time scales are now receiving broad attention in sciences and finance (e.g. [12,23]). When simulating such processes, it is desirable to consider the entire ensemble of all possible realizations rather than one realization. In practice, only a single realization is observed or measured and the ergodic hypothesis must be used to extrapolate the measured statistics from this realization to the ensemble behavior. Methodologies to construct plausible ensemble runs from a single realization are further complicated by nonlinear interactions among scales and in time. Hence, there is a clear need for statistical methods that generate an ensemble of realizations from a single run for processes that exhibit hierarchical information flow while preserving their internal dynamics and persistency. Resampling is frequently used to increase the statistical power in inferences, especially in hazard predictions ([30]). As an example [28] recently applied a bootstrap method to demonstrate that the increase in the rate of occurrence of extreme floods in the Elbe and Oder rivers over the past 80–150 years was absent. River flow is generally a hierarchical process with many modes of variability [36].

In this work, we propose a wavelet based resampling method for generating ensemble runs from a single realization using atmospheric surface layer (ASL) turbulence as a case study of a hierarchical process. The similarity between rough wall boundary layers and other hierarchical processes is gaining broad attention in numerous fields (including finance). For example, the recent similarities between the foreign exchange markets and ASL turbulence received much discussion and debate in physics and finance despite the lack of rigorous theoretical arguments connecting turbulence to financial market dynamics ([12,23,24,42,25]). The reason why ASL turbulence serves as a logical reference for such analogies is attributed to the fact that many hierarchical processes exhibit information flow from large to small scales, non-Gaussian statistics, intermittency, and multi-fractal properties. For the turbulent kinetic energy cascade, these specific attributes have been rigorously studied for more than 60 years and are now reasonably well quantified. Resampling ASL turbulence time series remains a challenge because such turbulence is *non-Gaussian*, *nonlinear*, and *long-memory* process. Hence, any methodology that can successfully resample ASL turbulence is likely to be successful at resampling a broad range of hierarchical processes. Finally, ASL turbulence is a logical choice for this work because *real-world ensembles* can be experimentally collected thereby permitting direct (and independent) testing of any proposed resampling method.

The original idea of bootstrap was developed in [9] for approximating the sampling distribution and the variance of many statistics under the assumption of independent and identical distributed (i.i.d) data. To achieve this purpose, synthetic data is generated by independently re-sampling (with replacement) from the original observations, their statistics of interest are computed, and the variance among the replicas is used to estimate the sample variance. The extension to non-i.i.d. time series data is not trivial and it usually depends both on the structure of the time series (in [35], the case of stationary time series is considered) and on the statistics of interest. To preserve the particular structure of the time series, block-resample, data dependent, or constrained re-sampling are often used (e.g. [28]). However, the performance of these strategies depends on two competing constraints: faithfully reproducing the statistics of the original observations, and producing sufficient variability among the surrogate series. Furthermore, recent efforts (see, for example [33]) for developing resampling methods for long memory processes typically transform the data into another domain (e.g. wavelets or Fourier based) that maximizes the decorrelation among coefficients. Bootstrap techniques based on the phase randomization in Fourier domain (hereafter referred to as FB) have been successfully applied ([40,37]) for generating surrogate time series. Recently, several wavelet surrogate methods have also been proposed (e.g. [3,4]). However, no study to date has compared the performance of the wavelet based resampling and FB to reconstruct ensemble statistics from a single experiment when measures of the ensemble are experimentally available. Hence, the main novelty of this work in the context of resampling methods for hierarchical processes are three-fold: (1) develop ad hoc wavelet based resampling strategy with block resampling (hereafter referred to as WB), (2) compare WB and FB using an ensemble of turbulence time series collected from two ASL field experiments,

and (3) extend the WB to multivariate time series and test it with multivariate ensemble turbulence time series in the ASL. Many limitations of resampling schemes discussed in [29] regarding uneven sampling and gaps can be partially resolved within the proposed WB.

The organization of this manuscript is as follows: the methodology for resampling hierarchical time series is described in Section 2. The application of WB to an idealized hierarchical (but linear) process such as fBm is discussed in Section 3. The application and comparison of FB and WB to two ASL turbulence experiments performed over different surfaces and meteorological conditions is described in Section 4. Conclusions and recommendations are presented in Section 5.

2. Resampling methods for hierarchical processes

2.1. General theory about bootstrap

The idea of the bootstrap is described as follows. Suppose that $\underline{X} = (X_1, \ldots, X_n)$ are n i.i.d. observations from an unknown distribution F and that one is interested in inferences on a parameter θ using the statistic $\hat{\theta} = T(X_1, \ldots, X_n)$. If the distribution of the statistics T is not known or requires a complicated mathematical expression, then one can generate B surrogate data $\underline{X}^b = (X_1^b, \ldots, X_n^b)$, $b = 1, \ldots, B$, by independently re-sampling with replacement in the observed vector $\underline{X}$, computing the statistic $\hat{\theta}^b = T(X_1^b, \ldots, X_n^b)$, and evaluating the accuracy of the statistic T by the standard deviation among the $\hat{\theta}^b$ estimates. Similar procedures can also be designed for computing confidence intervals (see [10,7], for a general review of the theory). When the observations exhibit some correlation, the naive approach of the bootstrap becomes ineffective and different re-sampling strategies that take into account both the stochastic structure of the data and the particular statistics of interest should be considered. The surrogate data must mimic the behavior of the observed data for most of the parameters of interest. This objective is usually achieved by placing some constraints on the re-sampling strategies such as using blocks of data (see, for example [21]).

2.2. Wavelet based resampling

Over the past 10 years, numerous studies have demonstrated the so called *de-correlating* property of the orthonormal wavelet transform, which is central to the concept of bootstrap (see, for example [15,16]). In fact, the correlation between the wavelet coefficients of many signals is usually small even if the signal itself is highly autocorrelated in the time domain [6,22,41]. In particular, it has been shown in [11,39] that the wavelet transform has optimal de-correlating property for the class of $(1/f)$-like signals; this is clearly expressed by the fact that the correlation between the wavelet coefficients $d_{j,k}$ and $d_{j',k'}$ at different levels behave as

$$\langle d_{j,k}, d_{j',k'} \rangle \sim O(|2^j k - 2^{j'} k'|^{2(H-L)}),$$

and between wavelet coefficients at the same levels as

$$\langle d_{j,k}, d_{j,k'} \rangle \sim O(|k - k'|^{2(H-L)}),$$

where L is the number of vanishing moments of the mother wavelet and H is the Hurst exponent. Additionally the wavelet coefficients are exactly stationary within each level for non-stationary processes with stationary increments (hence in particular for fBm processes), however such a property was approximately observed in few hierarchical processes including turbulence. We note that orthonormal wavelet transforms do not destroy the original correlation in the series; rather, this correlation is preserved through the scaling coefficients. In short, this de-correlation allows the development of resampling methods in the wavelet domain by:

(1) Applying an orthogonal wavelet transform to the observed time series.
(2) Generating surrogate wavelet coefficients using a suitable re-sampling strategy (described later).
(3) Applying the inverse wavelet transform to the re-sampled wavelet coefficients to generate a surrogate time series.

Regarding the re-sampling strategy, assume that $n = 2^J$ and the original time series $\underline{X} = (X_1, \ldots, X_n)$ is transformed up to the coarse level J_0 using an orthogonal wavelet basis with a finite number of vanishing moments. The choice of the number of vanishing

moments must be based on a compromise between the de-correlation property and the length of the filter. With these constraints and simplifications, the wavelet transform of the series yields $(c_{J_0,0}, \ldots, c_{J_0,2^{J_0}-1} d_{J_0,0}, \ldots, d_{J_0,2^{J_0}-1}, \ldots, d_{J-1,0}, \ldots, d_{J-1,2^{J-1}-1})$, where $c_{J_0,k}$ are the scaling coefficients and $d_{j,k}$ are the wavelet coefficients. To generate surrogate data, one can re-sample (with some ad hoc strategies) the wavelet coefficients d_{jk} within each level j and independently between the levels but retaining the coarsest coefficients $c_{J_0,k}$ unaltered. Finally, to obtain $\underline{X}^b$ it is sufficient to apply the inverse wavelet transform on $(c_{J_0,0}, \ldots, c_{J_0,2^{J_0}-1}, d^b_{J_0,0}, \ldots, d^b_{J_0,2^{J_0}-1} \ldots, d^b_{J-1,0}, \ldots, d^b_{J-1,2^{J-1}-1})$ for $b = 1, \ldots, B$. The unchanged coarsest scaling coefficients preserve the main features in the original signal (including global trends). We note that resampling each wavelet scale independently should not destroy the frequency content and the energy cascade. Several strategies on how to re-sample the wavelet coefficients within each level is discussed next.

The idea of resampling time series in the wavelet domain is not new. The simplest procedure is to independently re-sample wavelet coefficients one by one within each level (e.g. [3,4,33]). Resampling can be done with replacement like in the i.i.d. case or without replacement (i.e., permutation of wavelet coefficients). The best option depends on the particular features one wants to investigate. For example, resampling with replacement introduces variability in the energy or variance of the signal while permutation of coefficients preserves the energy precisely. Although the wavelet coefficients within a given level show a small autocorrelation, they are not strictly independent and hence the simplest procedure usually fails in producing synthetic data much less correlated with respect to the original data. Moreover, in this case, the spectral density of the surrogate data resembles white noise at small scales. Since the spectra and its decay are important features in hierarchical time series, these artificial effects are clearly unsatisfactory. The "whiteness of the spectra" is also described in [3] within the context of hypothesis testing.

To resample weakly correlated data within the wavelet domain, one can use a block-bootstrap approach to partially preserve the correlation structure. In its simplest version, block-bootstrap randomly resamples fixed-size blocks of wavelet coefficients within each level instead of each single coefficient. The performance of the methods depends on the choice of the block size (single coefficient resampling can be regarded a block method with block size unity). Larger blocks better preserve the correlation structure at the expense of reducing the number of possible realizations for surrogate data generation. Ideally the block size should be larger than the maximum lag for which the autocorrelation function is significant, however, from a practical point of view it is often empirically chosen. Finding the optimal block size in a "data dependent way" is usually difficult because it depends on the particular statistics to be preserved and the resampling approaches (overlapping or non-overlapping blocks; see [14,21]). Standard non-overlapping fixed size block based resampling in the wavelet domain are used in [3] for testing nonlinearity and the results compared with the ones obtained with the single coefficient approach, show significant improvements that can be considered satisfactory for many statistics. In contrast to the aforementioned fixed size block resampling scheme, the stationary bootstrap of [35] provides a methods for generating stationary synthetic data. In our context, assuming as in [13] that the wavelet coefficients within each level are almost stationary, it is natural to seek a resampling strategy that preserves stationarity. To achieve this purpose at each level $j \geq J_0$ and for each block, first a block size L_i is randomly sampled from the geometric distribution with parameter p_j, then the starting block position B_i is uniformly selected in $0, 1, \ldots, 2^j - 1$ and the block $d_{j,B_i}, \ldots, d_{j,B_i+L_i-1}$ is selected (periodic condition are used in wrapping the data). The selected blocks are concatenated to obtain the 2^j resampled wavelet coefficients $d^b_{j,0}, \ldots, d^b_{j,2^j-1}$. It has been shown in [14,35] that the choice $p_j \sim 2^{-j/3}$ is asymptotically optimal within each level as j increases, in the sense that such a choice minimizes the risk (the sum of the variance and the squared bias) of the estimate (at a given level). We observe that the optimal rate does not depend on the covariance structure as soon as the conditions given in Theorem 1 of [35] are satisfied. However, the constant c (i.e., $p_j = c\, 2^{-j/3}$) depends on the covariance of the process, and to a priori estimate the optimal constant is difficult in practical applications. In our simulation, the choice of c is fixed ($c = 0.25$) and was empirically

chosen after some tuning. We also found that any value of c between 0.25 and 0.50 provides almost indistinguishable results. Note that using such an approach, the mean block size of the selected blocks within the level j is $1/p_j$. Independent time series resampling is applied to each set of measurements to compute univariate based statistics. The performance of the univariate WB is also compared to FB to assess which of these two methods better preserves intermittency and non-Gaussian attributes of the turbulent energy cascade. The extension to the bivariate case, which is necessary to formulate resampling strategies of cross-statistics, can be obtained by performing the same set of permutations on the detailed coefficients of each time series.

2.3. Technical issues related to the resampling method

The choice of the wavelet family and the size of the filter are as important as the choice of the block size (or the mean block size). The de-correlating property implies that the correlation between wavelet coefficients decays rapidly with increasing number of vanishing moments of the wavelet filter. However, it should be noted that a filter with higher number of vanishing moments requires larger support. Increasing the width of the support of the wavelet function produces undesirable boundary artifacts in the surrogate data. The selection of the block size is equally important and requires a priori analysis. For this reason, we conducted a sensitivity analysis on both the filter influence and the block size.

To select the filter size and block size, we first considered spectral properties; these properties are central to any hierarchical process. Short filters or small block size in resampling methods often produce synthetic data with high frequency spectral behavior resembling white noise. This artificial effect is significant for the single coefficient resampling method but is less pronounced for the blocking methods. For the ASL turbulence data (described later), we found that filter sizes with six to eight vanishing moments and a block size of 32 are adequate to obtain physically acceptable surrogate data (see, Appendix A, for details).

We also conducted a similar sensitivity analysis on the probability distribution function of the synthetic time series. It is well known that random re-sampling produces synthetic data with almost Gaussian amplitude distribution. Block methods tend to minimize this drawback, but the Gaussianization phenomena cannot be eliminated without some adjustments. One adjustment procedure proposed in [40] is based on rank-order statistics and provides surrogate time series with the same pdf as the original one. This idea, used for phase randomization, can be easily extended to the wavelet resampling scheme here. However, this adjustment is not recommended for two reasons: first, it tends to introduce spurious white noise components on the spectrum, and second, it forces the pdf of the surrogate data to be identical to the original data. Experimentally, the pdf of turbulent signals measured under comparable meteorological conditions are "similar" but not identical. To reduce this gaussianization effect, we use the procedure proposed in [3]. In this procedure, a surrogate time series is accepted if the pdf is "close" to the pdf of the original time series. The less stringent constrain on the pdf can be used to judge the goodness of a resampling method as well. For example, counting the fraction of accepted surrogate time series generated by the method is one goodness measure (though not unique). A measure of closeness between pdfs can be the root mean squared difference between surrogate and observed pdfs (see [3], for a detailed description of the method). Surrogate time series selected with this approach show proper spectral density power law scaling and reduced "gaussianization".

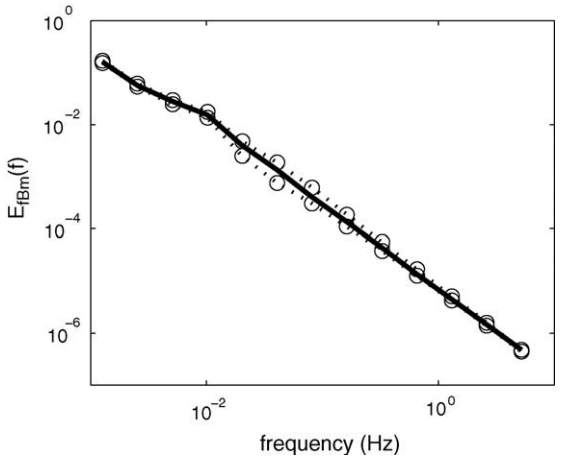

Fig. 1. The envelope of ensemble wavelet spectra (three standard deviations from the ensemble mean) computed from 500 WB time series along with the original fBm spectra (solid line).

3. Testing WB on a synthetic linear hierarchical process: a case study on fBm

An initial (but weak) validation of WB was carried out by analyzing the second order moment preservation of a simulated fractional Brownian motion (or fBm) process. For simplicity, the realizations of the fBm process were generated using the classical phase randomization algorithm to assure to correct frequency decay. The surrogate data are obtained using the wavelet stationary block resampling method described in Section 2.2 and Daubechies wavelet filter with 6 vanishing moments. Realizations from a fBm process with Hurst exponent 1/3 and length $n = 2^{15}$ where generated. This Hurst exponent was chosen because the resulting fBm spectrum has a power-law decay consistent with fine scale ASL turbulence. Starting from one fBm realization 500 synthetic series were generated and the power spectrum of each surrogate realization is shown in Fig. 1. As a reference, the power spectrum of the original fBm realization is also shown. This analysis demonstrates that the spectral agreement between the original fBm and the WB surrogate data is reasonably well. In particular, note that the choice of the wavelet stationary resampling scheme with a sufficiently large wavelet filter does not suffer from the so called 'whiteness of spectra' at the finest scales, a typical artifact common to several resampling strategies.

Table 1
Summary information about the cluster mean wind ($\langle U \rangle$) conditions, surface shear stress ($\langle u'w' \rangle$), sensible heat flux ($\langle H \rangle$), and atmospheric stability parameter (z/L) at each site

	$\langle U \rangle$ (ms^{-1})	$\langle u'w' \rangle$ (ms^{-1})^2	H (Wm^{-2})	z/L
Site 1	6.0 ± 0.2	-0.09 ± 0.01	11 ± 2	-0.04
Site 2	4.0 ± 0.2	-0.18 ± 0.04	45 ± 8	-0.03

The standard deviations around these cluster mean (or ensemble mean) values resulting from run to run variations are also shown.

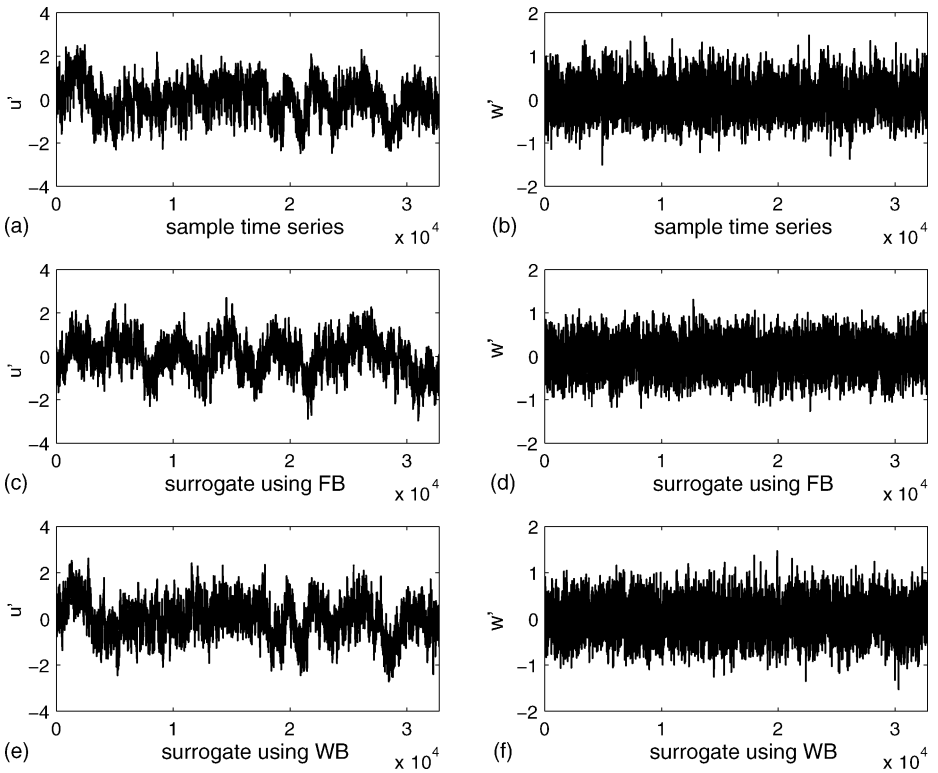

Fig. 2. Measured u' (a) and w' (b) time series taken from the cluster at Site 1. Sample surrogate time series for u' (c) and w' (d) generated by the FB, and sample surrogate time series for u' (e) and w' (f) generated using WB are shown. For the WB, Daubechies with six vanishing moments was used for the decomposition.

4. Application of the resampling methodology on atmospheric turbulence data

As earlier stated, ASL turbulence is commonly used as a case study for hierarchical processes that exhibit intermittent and non Gaussian energy cascades. The aforementioned wavelet resampling methodology here is applied to two different data sets. The first data set is from an experiment carried out at Terra Nova Bay, Antarctica, over a homogeneous snowy area of 50 km × 30 km, and at gently sloping ≈0.4% terrain (Site 1). The longitudinal (u') and vertical (w') turbulent velocities were sampled at 20.8 Hz and at a height $z = 10$ m above the snowy surface. The experiment produced more than 100 runs, each having a duration of 26.2 min (=2^{15} data points). More information about the site characteristics can be found in [5]. The second data set was collected above a grass surface at Duke Forest near Durham, North Carolina (Site 2). In this experiment, u' and w' were sampled at 56 Hz and at $z = 5.2$ m, and for a wide range of atmospheric stability (z/L) conditions, where L is the Obukhov length. This experiment produced 97 individual runs, each having a duration of 19.5 min (=2^{16} data points). More information about the site characteristics can be found in [17]. An *ensemble* was constructed for each experiment by first clustering all the runs collected under near-neutral atmospheric stability conditions (i.e. $|z/L| < 0.1$). Then, further clustering was performed for runs having comparable surface heating (H) and mean shear stress ($\langle u'w' \rangle$). These clusters can be thought of as independent realizations of the same experiment – which is what the synthetic data is attempting to generate from one single realization. To independently validate the performance of the resampling methodology, the statistical properties of the clusters (i.e. measured ensemble) and the synthetic time series (i.e. surrogate data ensemble) are compared. We

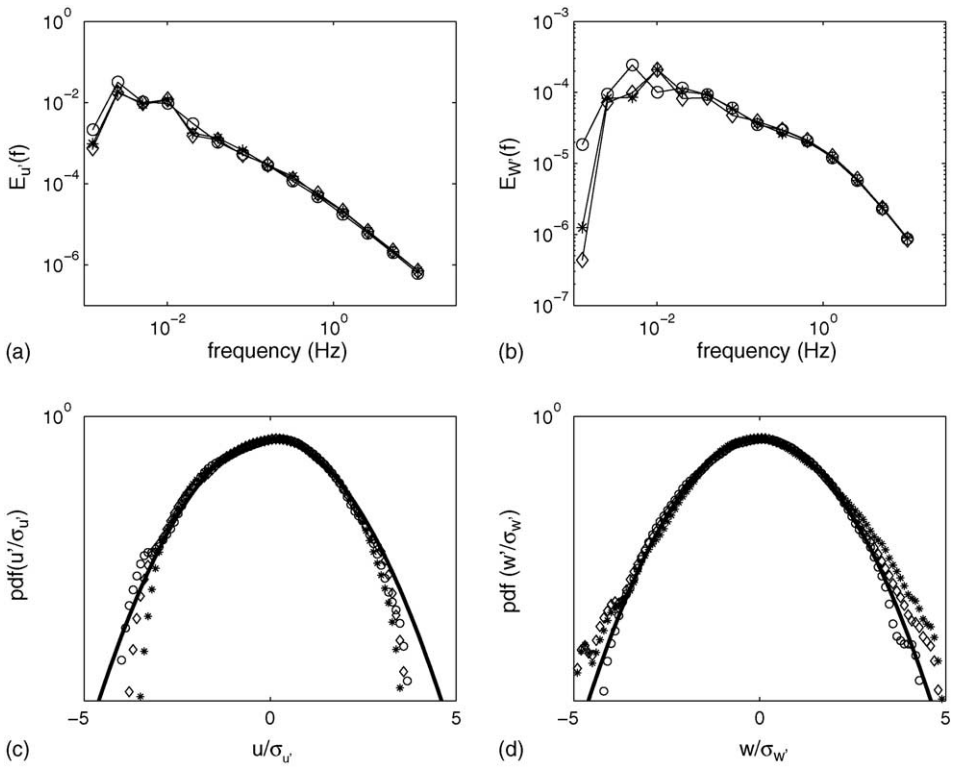

Fig. 3. Comparison between the measured and surrogate wavelet spectra of u' (a) and w' (b) for the series shown in Fig. 2. The corresponding pdf comparisons are also shown in (c) and (d). The different symbols refer to: measured time series (stars), surrogate time series generated by FB (circle), and surrogate time series generated using WB (diamonds). For reference, the pdf of a Gaussian process is also shown (solid line).

focus on a cluster of 10 runs for each of the two experiments. Information about the key statistics and the run to run variability within the cluster at each site can be found in Table 1. Fig. 2 shows a measured u' and w' time series at Site 1 (a and b) along with a randomly selected surrogate series generated from FB (c and d) and WB (e and f). From Fig. 2, it is clear that the synthetically produced and measured w' fluctuations appear less organized than their u' counterpart at the coarse scales. These differences are primarily due to mesoscale action and turbulence generation mechanisms in the different components. Within the inertial subrange (i.e. at scales much smaller than the integral time scale), the u' and w' statistical properties are dynamically (and statistically) similar due to the action of vortex stretching. That is, after many cascade steps, the ASL turbulence statistics become locally homogeneous and isotropic ([31]). Since the interest here is primarily in turbulent fluctuations within this energy cascade, the resampling strategy must not alter the mesoscale conditions. Hence, the coarsest levels (or scales) unaltered by the resampling must be estimated a priori. We choose the peak of the observed energy spectrum as an indication of the most energetic turbulent eddies and assume that eddies larger than these scales are mesoscale. With this separation between mesoscale and turbulence, the resampling method changes all wavelet coefficients finer (and including) the most energetic level.

To illustrate the differences between the synthetic and measured time series in Fig. 2, spectral and pdf comparisons are conducted in Fig. 3. This comparison suggests that both methods preserve the spectral properties of the original time series and similar results hold

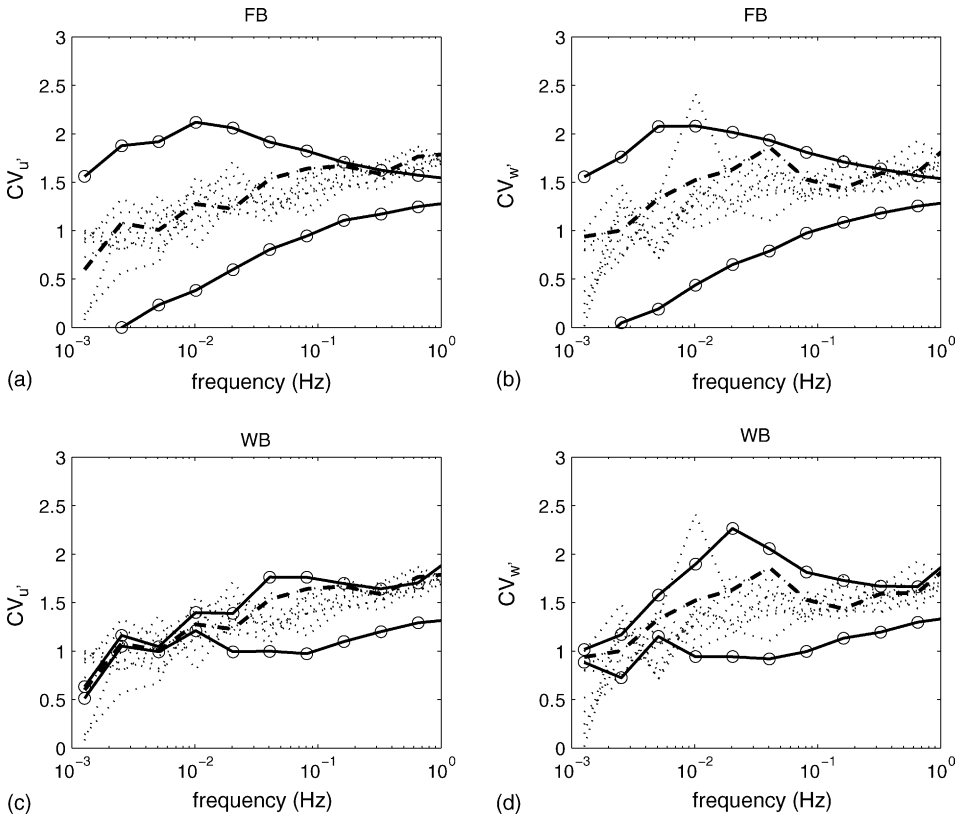

Fig. 4. CV of the cluster for u' and w' for Site 1 along with the CV of the surrogate data generated by FB (a and b) and by WB (c and d). Dot-dashed lines refer to CVs of the whole cluster, while the dashed black line represent the CV of the reference time series used when resampling. Finally open circles and lines represent the envelope of ensemble CV (three standard deviations from the ensemble mean) computed over 500 synthetic runs.

when changing the original time series or the surrogate sample. By contrast, the simple comparison of pdfs is not sufficient to highlight the differences between the FB and the WB strategies since the shape of the pdfs shows higher variability respect to the choice of the time series and the surrogate samples, hence more accurate parameters must be used for this purpose. A time series from the ensemble of 10 runs for each experimental site is chosen for generating 500 surrogate time series runs (per experimental site). When resampling, simultaneously matching the spectra and pdf of the original series cannot be achieved exactly. We followed [3] who proposed that a synthetic run is accepted only if its pdf is sufficiently close to the pdf of the original time series. Root mean squared difference between the histogram of the measured time series and the candidate surrogate series is computed and the candidate series is accepted if the difference is within 10–15%. Not forcing the pdfs of the original and surrogate data to precisely match each other reduces spurious artifacts such as the 'whiteness of the spectra'. On the other hand, not allowing substantial changes in the pdf retains realizable surrogates. We note that with proper tuning of parameters such as filter size and coarsest wavelet level, the numbers of rejected surrogate runs is, in many cases, negligible when wavelet stationary resampling is used along with a suitable choice of the filter size to de-correlate the data. A preliminary analysis of the clustered time series at both sites shows that while the spectra of u' and w' within the inertial subrange were almost identical, the pdfs were not. Hence, the stringent constraint to match in resampling must be the spectrum not the pdf. While the analysis in Fig. 3 suggests that both WB and FB reproduce reasonably well the statistics of an individual realization, no information about intermittency preservation in the series is provided. Hence, a stronger support for using WB vis-a-vis FB can be obtained by assessing how well these two resampling methodologies reproduce the ensemble cluster. We consider the following measures of

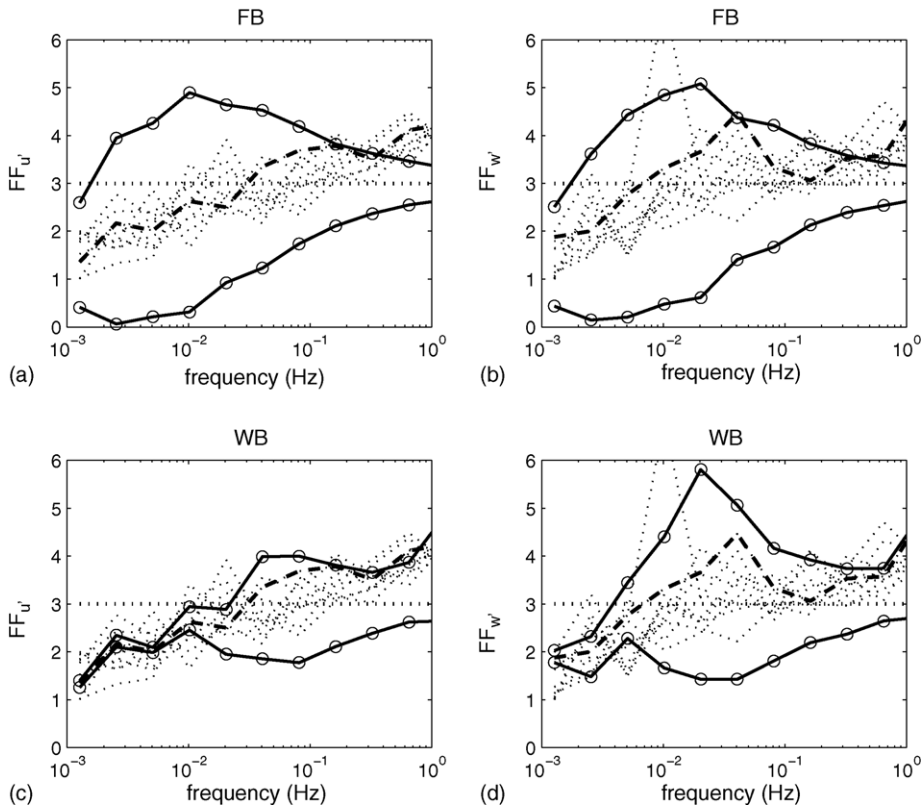

Fig. 5. As in Fig. 4, but for FF. The horizontal dotted line represents the 'Gaussian value' of FF.

intermittency in the wavelet domain at each scale index:

(1) Coefficient of variation of energy, $\mathrm{CV}_j = \frac{[\langle d_{j,k}^4\rangle - \langle d_{j,k}^2\rangle^2]^{1/2}}{\langle d_{j,k}^2\rangle}$,

(2) Flatness factor, $\mathrm{FF}_j = \frac{\langle d_{j,k}^4\rangle}{\langle d_{j,k}^2\rangle^2}$.

CV is a good indicator of the spatial energy variance, whereas FF (whose 'Gaussian value' is 3) measures the importance of the tails of the probability density function of the velocity differences. Both measures are expected to increase with increasing frequency in the turbulent cascade, as consequence of the increased intermittency in the dissipation rate at small scales (e.g. [18]). Fig. 4 shows the CV of the cluster for u' and w' for Site 1 along with the CV of the surrogate data generated by FB and WB. It is clear from Fig. 4 that both resampling methods underestimate the scale-wise evolution of the cluster CV. While the FB exhibited little variation in CV with increasing frequencies, the WB showed some increase in CV. Hence, Fig. 4 suggests that WB partially (not fully) preserves the intermittency while FB destroys all the intermittency. This behavior is further confirmed by the FF in Fig. 5. The FF for FB are nearly Gaussian across the inertial subrange, while WB resulted in an FF that increases beyond its Gaussian value (=3) with increasing frequency. These preliminary results suggest that WB does not destroy the intermittency within the energy cascade. The logical next step is to assess whether WB preserves the multifractal properties of the turbulent energy cascade. One approach to assess the multifractal properties of the energy cascade is the scaling behavior of pth order structure function ($p = 1, 2, \ldots, 10$),

$$S_p = \langle [u(x+r) - u(x)]^p \rangle \propto r^{\zeta_p}.$$

The main characteristics of intermittent signals that display a multiplicative cascading structure is the existence of long-range correlations [32,1]; therefore, the structure function approach is often used as a method for quantifying the effects of intermittency on the flow dynamics and its dependence on scale. Briefly, the departure of the scaling exponents from K41 theory [19], $\zeta_p = p/3$, have been classically attributed to intermittency in the turbulent kinetic energy dissipation rate. Hence, the presence of intermittency at fine scales may be evaluated by the 'anomalous' scaling exponents, that is from the non-linear dependence of ζ_p over p. Fig. 6 shows ζ_p of the cluster for u and w structure functions for Site 1 along with ζ_p for u and w structure functions of the surrogate data generated

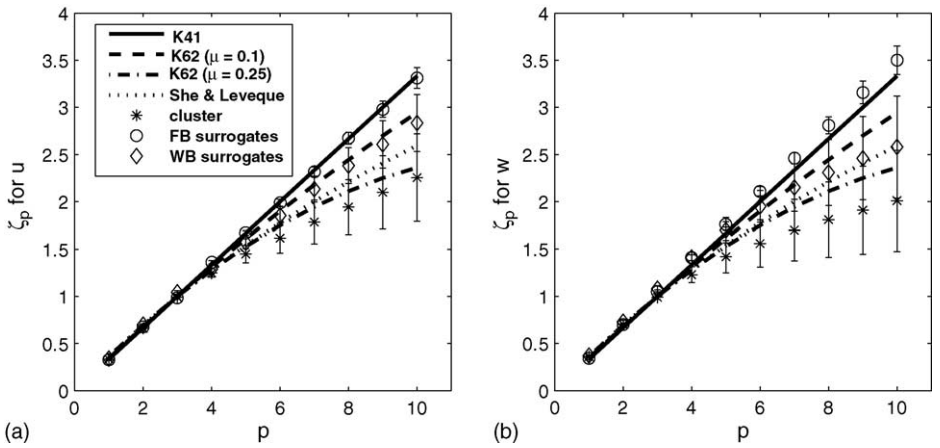

Fig. 6. Scaling exponents, ζ_p of the cluster (stars) for u (a) and w (b) structure functions for Site 1 along with ζ_p for u and w structure functions of the surrogate data generated by FB (circles) and WB (diamonds). The symbols represent the average values, whereas the vertical bars represent three standard deviations from the mean. Finally, for reference we show the K41 model [19] (solid line), the K62 model [20] with $\mu = 0.1$ (dashed line) and $\mu = 0.25$ (dot-dashed line), and the She-Levêque model [38] (dotted line). The structure functions are computed in the wavelet domain according to the formulation in [18].

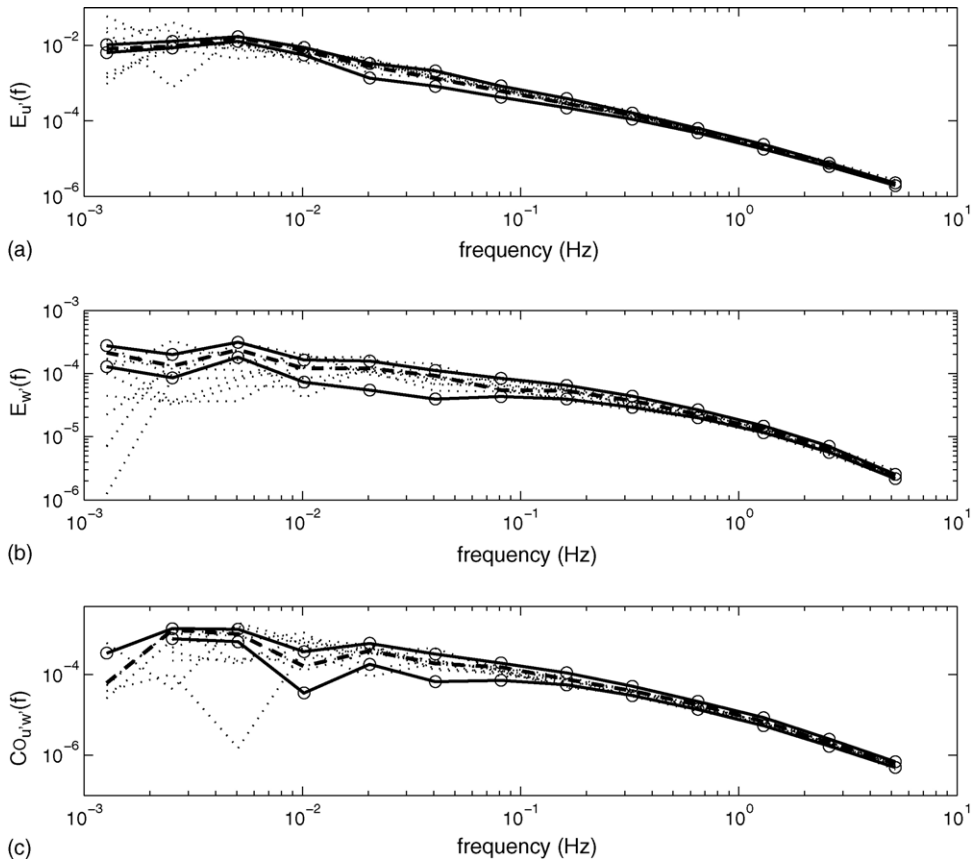

Fig. 7. The wavelet based u' spectrum (a), the w' spectrum (b) and the $u'w'$ cospectrum (c) of the cluster for Site 1 along with the corresponding quantities of the surrogate data by wavelet based resampling. Dot-dashed lines refer to spectra and cospectrum of the whole cluster, while the dashed black line represent the spectra and cospectra of the reference time series used when resampling. Finally open circles and lines represent the envelope of ensemble spectra and cospectra (3 standard deviations from the ensemble mean) computed over 500 synthetic runs.

by FB and WB. The structure functions have been computed in the wavelet domain, using the differencing characteristics of the Haar wavelet that allow an explicit relationship between the structure functions and the wavelet coefficients (see [18], for further details). For reference, the K41 model [19], the K62 model [20] with intermittency exponents $\mu = 0.1$ and 0.25, and the She-Levêque model [38] are shown. It is evident that for both velocity components, the scaling exponents derived from FB surrogates follow K41 theory (solid line) suggesting complete intermittency suppression (as expected). On the other hand, Fig. 6 confirms that WB preserves some of the small scale intermittency, although partially reduced. While Figs. 4–6 show the results for Site 1, the same analysis was

Table 2
Comparison between measured and WB surrogate data mean (and std) spectral and co-spectral exponents within the inertial subrange

Variable/site	Cluster ensemble measured exponents	WB ensemble computed exponents
u' spectrum on Site 1	−1.656 (0.013)	−1.673 (0.017)
w' spectrum on Site 1	−1.703 (0.020)	−1.711 (0.025)
$u'w'$ co-spectrum on Site 1	−2.334 (0.469)	−2.076 (0.220)
u' spectrum on Site 2	−1.586 (0.017)	−1.596 (0.017)
w' spectrum on Site 2	−1.378 (0.027)	−1.417 (0.025)
$u'w'$ cospectrum on Site 2	−1.923 (0.055)	−1.897 (0.052)

The measured slopes are based, at each site, on the 10 runs within each cluster and on the 500 WB surrogates.

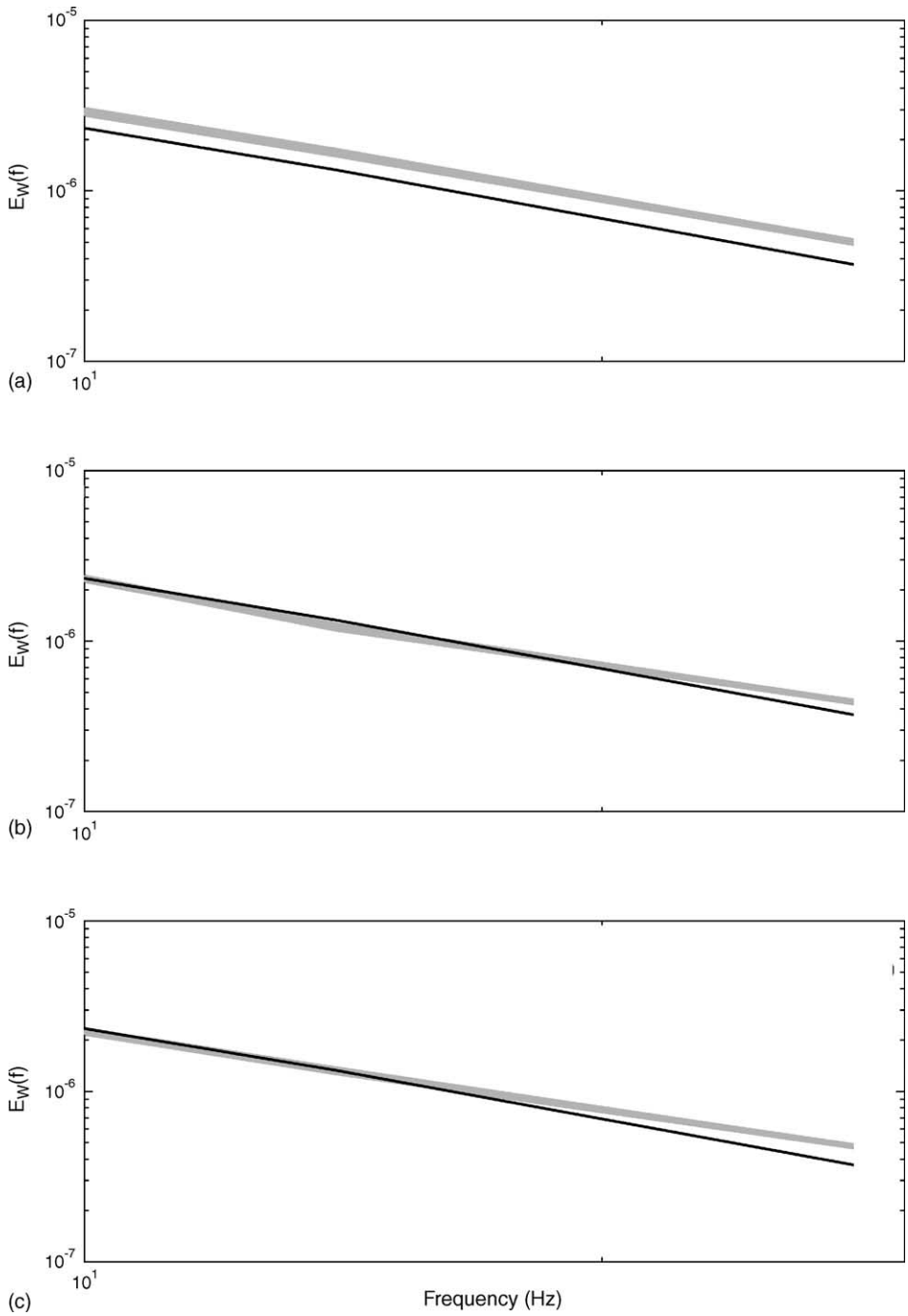

Fig. 8. Power spectrum in the range 10–30 Hz of 50 synthetic time series obtained resampling every wavelet coefficient of the selected time series measured on Site 2 independently levels by levels. Panels (a–c) refer to the choice of the filter support (taken as Daubechies type) with 2, 6, and 10 vanishing moments, respectively.

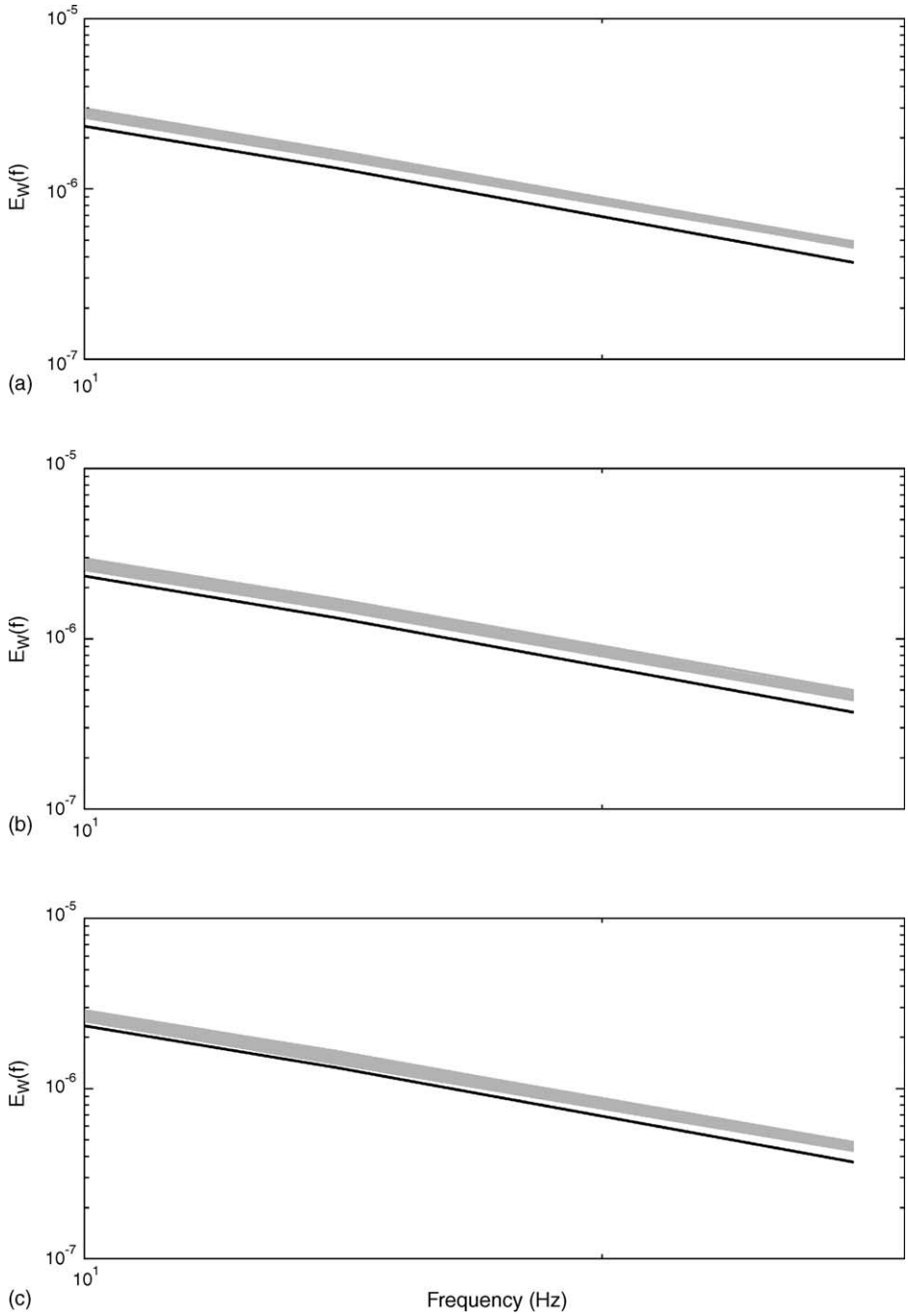

Fig. 9. As in Fig. 8, but for non-overlapping blocks resampling strategy. Blocks of length 4, 16 and 64 are considered (a–c, respectively). The Daubechies wavelet with 2 vanishing moments is used when resampling.

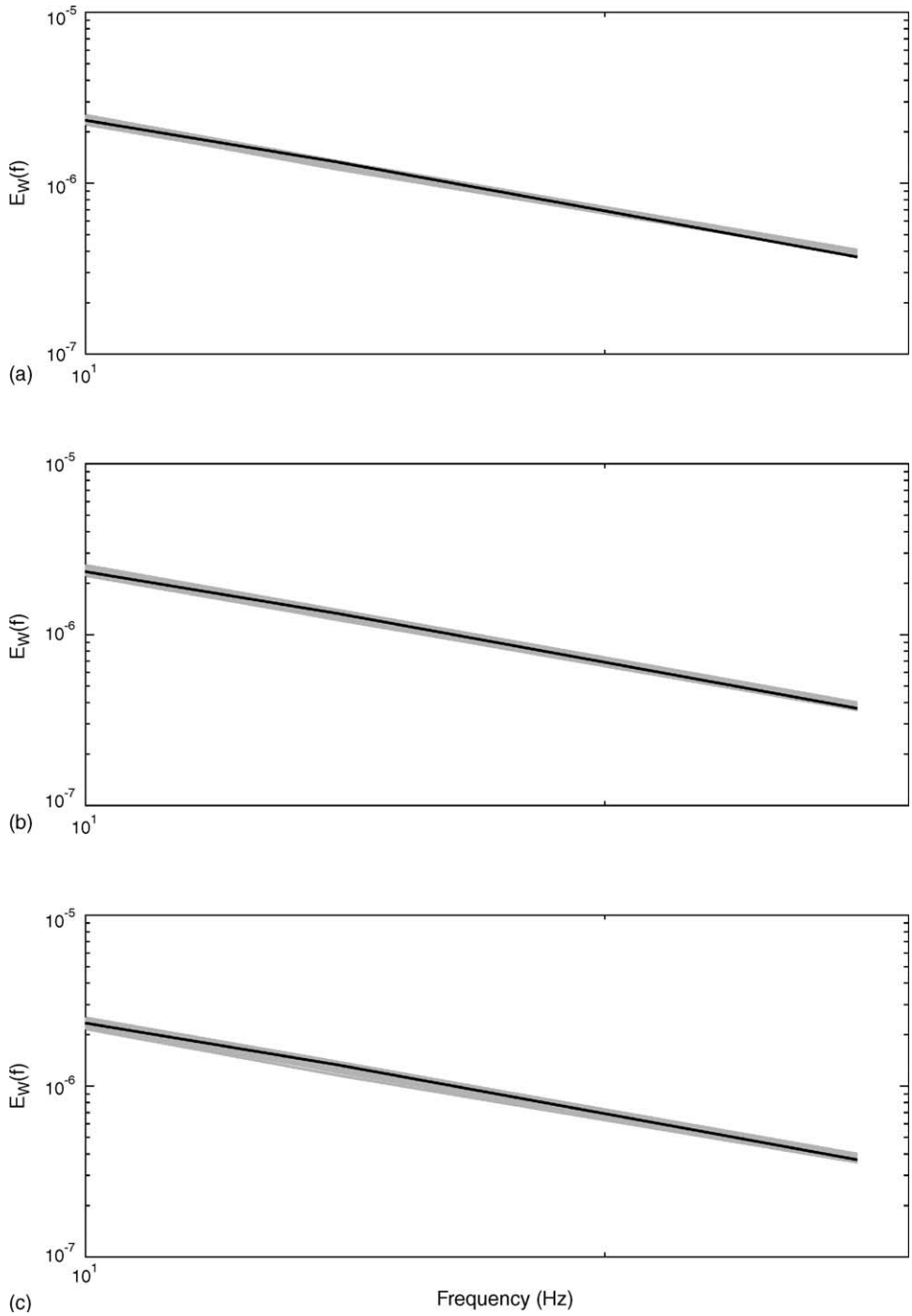

Fig. 10. As in Fig. 9 but Daubechies wavelet with 6 vanishing moments is used when resampling.

repeated for Site 2 with similar findings (figures not shown).

Finally, the proposed WB method can be readily extended to multivariate data to compute cross statistics such as the co-spectrum C_{uw}. To preserve the local correlations among the multivariate data, this extension is achieved by performing the same set of random permutations to the detailed wavelet coefficients of each time series. In Fig. 7, we show the co-spectra C_{uw} computed for the cluster time series for Site 1 along with the WB surrogates. Analysis of the figure shows that the co-spectra computed using the surrogate time series mimic the cluster co-spectra, and the spread of the synthetic data can be used to asses the variability of the cluster co-spectra when only one realization is used. A typical measure of interest in the spectral and co-spectral analysis is the exponent in the inertial subrange. Table 2 shows the exponent and the standard deviation (computed both on the cluster and on the 500 WB realization) of the spectra and C_{uw} within the inertial subrange for both experimental sites. The analysis in the table support the aforementioned results.

5. Conclusions

Numerous studies pointed out to the need for developing statistical methods that generate an ensemble of realizations from a single run for hierarchical time series. As discussed in [29], developing resampling methodologies for (1) unevenly spaced multidimensional time series, and (2) incorporating time-scale uncertainties in the re-sampling procedures is becoming crucial in inference testing for climate change research. Turbulence serves as a common phenomenological process for many hierarchical processes in sciences and finance and hence serves as a logical test for resampling methodologies. This phenomenological analogy to turbulence is commonly invoked because many hierarchical processes exhibit information flow from large to small scales, non-Gaussian statistics, and intermittency. These attributes are defining elements of the well-studied turbulent energy cascade.

In this study, a wavelet based resampling scheme that can accommodate both features is compared to the traditional Fourier based phase randomization bootstrapping within the context of a turbulent kinetic energy cascade. The wavelet domain can readily accommodate unevenly spaced time series [16]. Data sets from atmospheric surface layer turbulence experiments were used to construct clusters of time series ensembles, and resampling was applied to one of these time series with the aim of reproducing the cluster (or ensemble) statistics. Given that the cluster ensemble spectra shows little variations, while the cluster pdf shows some variations, the wavelet resampling method was forced to match the spectrum and to within 15% the sample pdf. The comparison between the two resampling methods and the ensemble data demonstrated that the stationary wavelet method reproduces several features related to intermittency of the turbulence cascade when compared to the Fourier phase randomization. In particular, the wavelet based surrogate runs do exhibit an increase in energy activity and in non-Gaussianity with increasing frequency consistent with the cluster ensemble; moreover the 'anomalous' behaviour of the scaling exponents of the velocity structure functions confirms that WB retains some of the small scale intermittency buildup but not all of it. The Fourier phase randomization bootstrap yielded no increase in energy activity with scale, near Gaussianity at all frequencies within the inertial subrange, and 'normal' scaling coefficients following the K41 model [19]. The extension of the wavelet based resampling approach to the multivariate case is demonstrated via the conservation of the co-spectra between longitudinal and vertical velocity time series. It was shown that the variability of the wavelet based surrogate co-spectra, generated from 500 runs, is consistent with the co-spectral variability observed within the cluster.

Finally, we end this study with several cautionary comments about WB. We showed that the intermittency corrections to K41, often formulated in terms of $\overline{(\Delta u)^p} = C_p r^{\xi_p}$ were not precisely captured. For example, we showed that when the log-normal model $\xi_p = p/3 + \mu/18(3p - p^2)$ is fitted to the cluster data and the WB surrogates, the resulting μ were 0.25 and 0.1, respectively. That is, the nonlinearities in ξ_p beyond $p/3$ were clearly damped by WB by more than a factor of 2. Despite this dampening, WB remains a major advancement over FB that yielded a $\mu = 0$ (as expected). Furthermore, the randomization of wavelet coefficients across blocks and between scales in WB leads to an artifical rapid decay in the space-scale correlation function with distance for inertial subrange scales. This long-range dependence of the space-scale correlation

function has been shown to play a significant dynamical role in the turbulence cascade ([1,2,8,26,27]). Future efforts to improve WB may consider a wavelet-based re-sampling scheme that uses a two-dimensional window (in space and scale) so as retain canonical features of the space-scale correlation function decay. Depending on the duration of the experiment, this criteria will likely *compete* with the need to produce sufficient variability among the surrogate series in boot-strapping.

Acknowledgements

The authors thank D. Poggi for the helpful discussion about the surrogate data generation in [37] and for sharing with us an earlier version of his manuscript (in [34]). Also, the authors thank both referees for the helpful suggestions and comments, and particularly referee 1 for suggesting the analysis and validation for the *p*th order structure function. Cava acknowledges the CNR for the SHORT-TERM MOBILITY Programme, 2004, and the support of the CNR-ISAC for the Project 'Effetti delle Strutture Coerenti sul Trasporto Turbolento in Canopy Vegetale' (Progetto Giovani Ricercatori CNR-ISAC, 2003). Katul acknowledges the support of the US National Science Foundation (NSF-EAR-02-08258 and NSF-DMS-00-72585), the Biological and Environmental Research (BER) Program, U.S. Department of Energy, through the Southeast Regional Center (SERC) of the National Institute for Global Environmental Change (NIGEC), and through the Terrestrial Carbon Processes Program (TCP) and the FACE project.

Appendix A. Sensitivity analysis to the filter size and wavelet resampling methods

We pointed out in Section 2.3 that the wavelet filter and block size are fundamental to the success of the overall wavelet resampling strategy. In this appendix, we present a sensitivity analysis on the block size and wavelet support using a w' series collected at Site 2 as an example. Fig. 8 shows the power spectrum zoomed in the range 10–30 Hz of 50 surrogate time series obtained with a block size of unity (i.e. resampling every wavelet coefficient). Panels (a–c) refer to the choice of the filter support (taken as Daubechies type) with 2, 6, and 10 vanishing moments respectively. Analysis of the figure shows some distortion of the power spectrum in the inertial subrange toward white noise (this drawback is significant when inspecting the power spectra in the Fourier domain). This whitening is a typical drawback of several re-sampling strategies when applied to highly structured data.

Turbulence time series are characterized by large integral time scales and the wavelet transform does not completely remove the correlation among coefficients within the same level; hence the independent term-by-term wavelet resampling is not satisfactory. Fig. 9 shows the spectra computed for the same sample using fixed length non-overlapping blocks resampling strategy. Blocks of length 4, 16 and 64 are considered (a–c, respectively) to preserve the correlation structure among the wavelet coefficients. The Daubechies wavelet with two vanishing moments is used to decorrelate the data. Fig. 10 repeats Fig. 9 but using a Daubechies wavelet with six vanishing moments. Comparing these two figures demonstrates that increasing the block size reduces the whiteness of the power spectrum. For this reason, wavelet filter size with six to eight vanishing moments are recommended; further increase in the wavelet support does not provide significant advantages. In short, block based methods outperform term-by-term re-sampling methods because they preserve the within level correlations. For the two experiments here, we found that using a Daubechies wavelet with six vanishing moments along with a fixed block length of 32–64 are quite satisfactory to reproduce the spectra.

References

[1] A. Arneodo, E. Bacry, S. Manneville, J.F. Muzy, Analysis of random cascades using space-scale correlation functions, Phys. Rev. Lett. 80 (1998) 708–711.

[2] A. Arneodo, S. Manneville, J.F. Muzy, S.G. Roux, Revealing a lognormal cascading process in turbulent velocity statistics with wavelet analysis, Phil. Trans. R. Soc. Lond. A 357 (1999) 2415–2438.

[3] M. Breakspear, M. Brammer, P.A. Robinson, Construction of multivariate surrogate sets from nonlinear data using the wavelet transform, Physica D 182 (1–2) (2003) 1–22.

[4] E. Bullmore, C. Long, J. Suckling, J. Fadili, G. Calvert, F. Zelaya, T.A. Carpenter, M. Brammer, Colored noise and computational inference in neurophysiological (fMRI) time series anal-

ysis: resampling methods in time and wavelet domains, Hum. Brain Mapp. Feb. 12 (2) (2001) 61–78.
[5] D. Cava, U. Giostra, M. Tagliazucca, Spectral maxima in a perturbed stable boundary layer, Boundary-Layer Meteorol. 100 (2001) 421–437.
[6] I. Daubechies, Ten Lectures on Wavelets, SIAM, Philadelphia, 1992.
[7] A.C. Davison, D.V. Hinkley, Bootstrap methods and their application, Cambridge Series on Statistical and Probabilistic Mathematics, vol. 1, Cambridge University Press, Cambridge, 1997.
[8] J. Delour, J.F. Muzy, A. Arneodo, Intermittency of 1D velocity spatial profiles in turbulence: a magnitude cumulant analysis, Eur. Phys. J.B. 23 (2001) 243–248.
[9] B. Efron, Bootstrap methods: Another look at the jackknife, Ann. Stat. 7 (1979) 1–26.
[10] B. Efron, R.J. Tibshirani, An introduction to the bootstrap, Monographs on Statistics and Applied Probability, vol. 57, Chapman & Hall, New York, NY, 1993.
[11] P. Flandrin, Wavelet analysis and synthesis of fractional Brownian motion, IEEE Trans. Inform. Theory 38 (1992) 910–917.
[12] S. Ghashghaie, W. Breymann, J. Peinke, P. Talkner, Y. Dodge, Turbulent cascades in foreign exchange markets, Nature 381 (1996) 767–770.
[13] S. Golia, Evaluating the GPH estimator via bootstrap technique, in: W. Hardle, B. Ronz (Eds.), Proceedings in Computational Statistics COMPSTAT2002, Physica-Verlag, Heidelberg, 2002, pp. 343–348.
[14] P. Hall, J.L. Horowitz, B.Y. Jing, On blocking rules for the bootstrap with dependent data, Biometrika 82 (1995) 561–574.
[15] G.G. Katul, B. Vidakovic, J.D. Albertson, Estimating global and local scaling exponents in turbulent flows using wavelet transformations, Phys. Fluids 13 (2001) 241–250.
[16] G.G. Katul, C.T. Lai, K. Schafer, B. Vidakovic, J.D. Albertson, D. Ellsworth, R. Oren, Multiscale analysis of vegetation surface fluxes: from seconds to years, Adv. Water Res. 24 (2001) 1119–1132.
[17] G.G. Katul, C.I. Hsieh, J. Sigmon, Energy-inertial scale interaction for temperature and velocity in the unstable surface layer, Boundary-Layer Meteorol. 82 (1997) 49–80.
[18] G.G. Katul, M.B. Parlange, C.R. Chu, Intermittency, local isotropy, and non-Gaussian statistics in atmospheric surface layer turbulence, Phys. Fluids 6 (1994) 2480–2492.
[19] A.N. Kolmogorov, The local structure of turbulence in incompressible viscous fluid for very large Reynolds number, Dokl. Acad. Nauk. SSSR 30 (1941) 9–13.
[20] A.N. Kolmogorov, A refinement of previous hypothesis concerning the local structure of turbulence in a viscous incompressible fluid at high Reynolds number, J. Fluid Mech. 13 (1962) 82–85.
[21] Lahiri, S.N. (2003). Resampling methods for dependent data. Springer Series in Statistics.
[22] S. Mallat, A Wavelet Tour of Signal Processing, Academic Press, London, 1999.
[23] R.N. Mantegna, H.E. Stanley, Turbulence and financial markets, Nature 383 (1996) 587–588.
[24] R.N. Mantegna, H.E. Stanley, Stock market dynamics and turbulence: parallel analysis of fluctuation phenomena, Physica A 239 (1997) 255–266.
[25] J.L. McCauley, Scaling, correlations, and cascades in finance and turbulence, Physica A 329 (2003) 213–221.
[26] N. Mordant, J. Delour, Leveque, A. Arneodo, J.-F. Pinton, Long time correaltions in Lagrangian dynamics: a key to intermittency in turbulence, Physical Review Letters 89 (1–4) (2002) 254–502.
[27] N. Mordant, J. Delour, E. Leveque, O. Michel, A. Arneodo, J.-F. Pinton, Lagrangian velocity fluctuations in fully developed turbulence: scaling, intermittency, and dynamics, J. Stat. Phys. 113 (2003) 701–717.
[28] M. Mudelsee, M. Börngen, G. Tetzlaff, U. Grünewald, No upward trends in the occurrence of extreme floods in central Europe, Nature 425 (2003) 166–169.
[29] M. Mudelsee, Bootstrap time series analysis, or how accurately can we quantify climatic changes? Earth, Fire, Water, Air and Life-Changing Earth and its impact on Human Habitat Research Conference, 4–6 April 2004, Washington, DC, German Research Foundation, 2004.
[30] J. Murray, P. Segal, Testing time-predictable earthquake recurrence by direct measurement of strain accumulation and release, Nature 419 (2002) 287–291.
[31] A.S. Monin, A.M. Yaglom, Statistical Fluid Mechanics, The MIT Press, Cambridge, 1971.
[32] J. O'Neil, C. Meneveau, Spatial correlations in turbulence: predictions from the multifractal formalism and comparison with experiments, Phys. Fluids A 5 (1992) 158–172.
[33] D.B. Percival, S. Sardy, A.C. Davison, Wavestrapping time series: adaptive wavelet-based bootstrapping, in: W.J. Fitzgerald, R.L. Smith, A.T. Walden, P.C. Young (Eds.), Nonlinear and Nonstationary Signal Processing, Cambridge University Press, 2001.
[34] D. Poggi, A. Porporato, L. Ridolfi, J.D. Albertson, G.G. Katul, Interaction between large and small scales in the canopy sublayer, Geophys. Res. Lett. 31 (5) (2004) L05102.
[35] D. Politis, J.P. Romano, The stationary bootstrap, J. Am. Stat. Assoc. 89 (428) (1994) 1303–1313.
[36] A. Porporato, L. Ridolfi, Multivariate nonlinear prediction of river flows, J. Hydrol. 248 (1–4) (JUL 15, 2001) 109–122.
[37] T. Schreiber, A. Schmitz, Surrogate time series, Physica D 142 (3–4) (2000) 346–382.
[38] Z.S. She, Levêque, Universal scaling laws in fully developed turbulence, Phys. Rev. Lett. 72 (1994) 336–339.
[39] A.H. Tewfik, M. Kim, Correlation structure of the discrete wavelet coefficients of fractional Brownian motion, IEEE Trans. Inform. Theory 38 (1992) 904–909.
[40] J. Theiler, S. Eubank, A. Longtin, B. Galdrikian, J. Farmer, Testing for nonlinearity in time series: the method of surrogate data, Physica D 58 (1992) 77–94.
[41] B. Vidakovic, Statistical Modeling by Wavelets, John Wiley & Sons, New York, 1999.
[42] J. Voit, From Brownian motion to operational risk: statistical physics and financial markets, Physica A 321 (2002) 286–299.